

Supporting Information for

The Glucocorticoid Receptor Potentiates Aldosterone-Induced Transcription by the Mineralocorticoid Receptor.

Thomas A. Johnson, Gregory Fettweis, Kaustubh Wagh, Diego Ceacero-Heras, Manan Krishnamurthy, Fermín Sánchez de Medina, Olga Martínez-Augustín, Arpita Upadhyaya, Gordon L. Hager, Diego Alvarez de la Rosa

Corresponding authors: GLH and DAdIR.

Email: hagerg@dce41.nci.nih.gov; dalrosa@ull.edu.es.

This PDF file includes:

Figures S1 to S6

Tables S1 to S2

Other supporting materials for this manuscript include the following:

Datasets D1 to D3

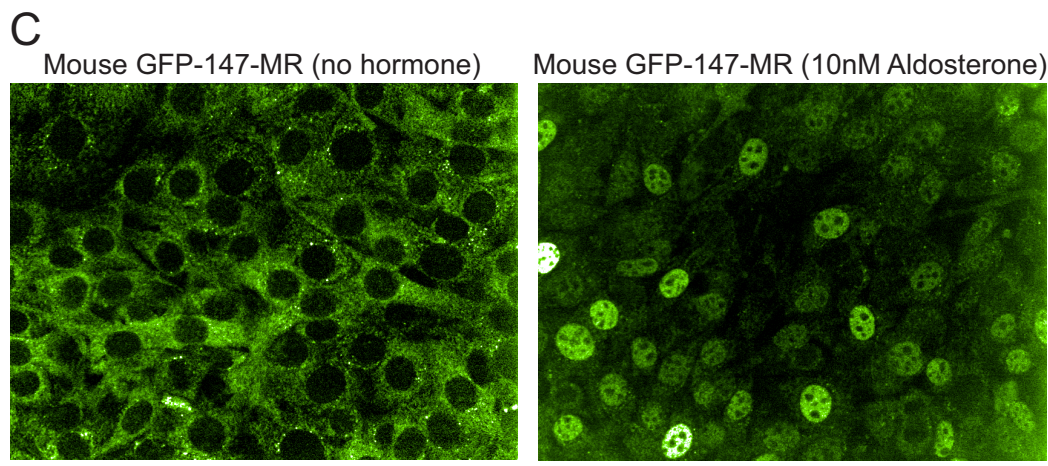
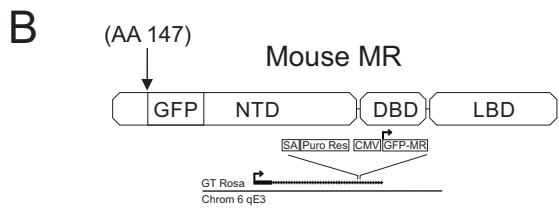
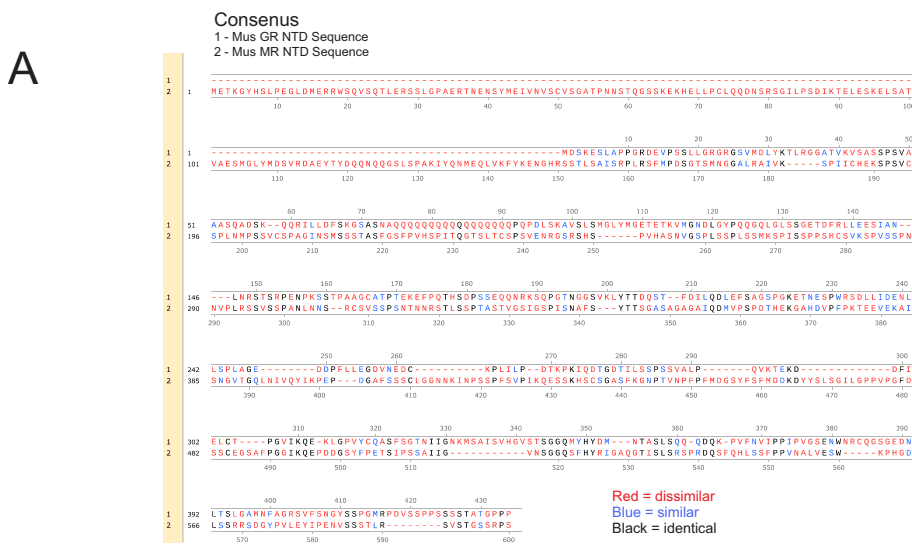


Figure S1. A. Sequence comparison between *M. musculus* MR and GR NTD. **B.** Schematic representation of *M. musculus* MR indicating the eGFP insertion site and the structure of the Donor-Rosa26_Puro_CMV-eGFP-MR vector. **C.** Representative confocal images showing eGFP-MR expression in a stable cell line and nuclear translocation after 1h 10 nM aldosterone treatment.

Fig. S2A

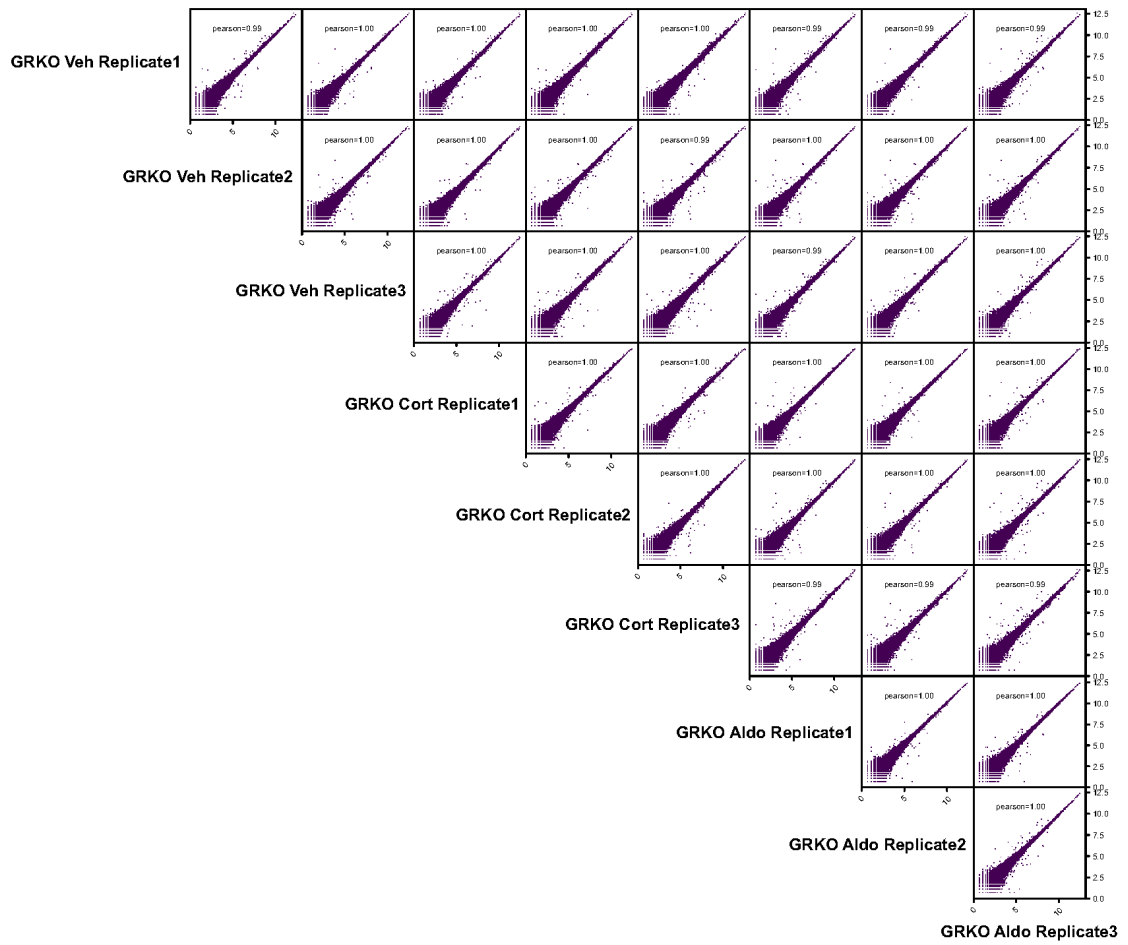


Fig. S2B

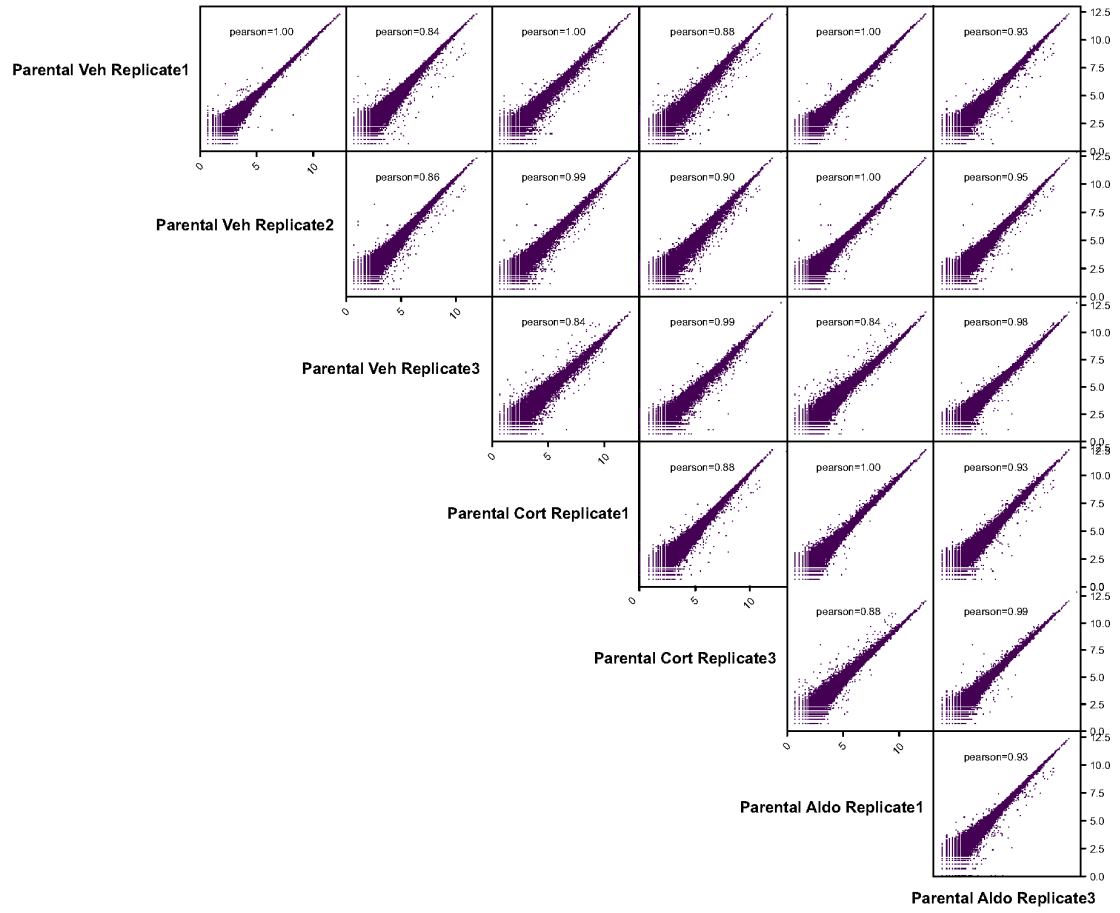


Fig. S2C

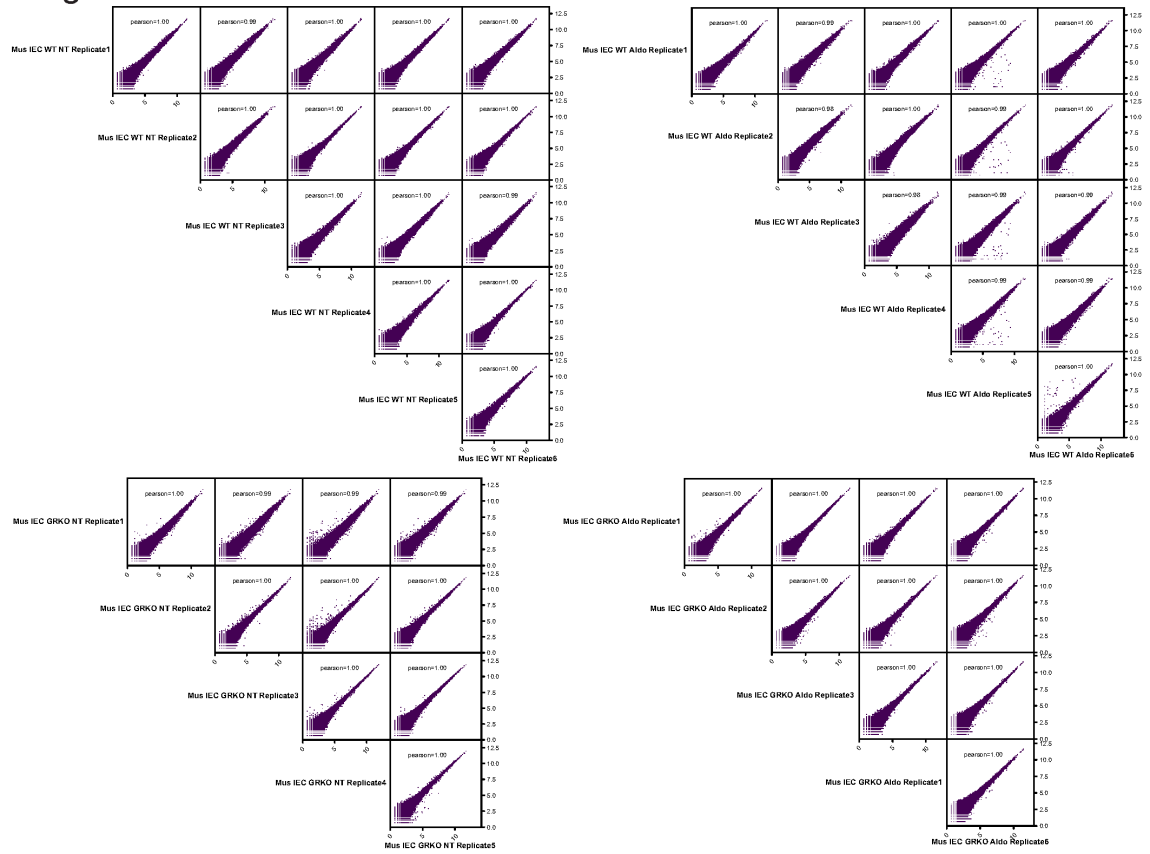


Fig. S2D

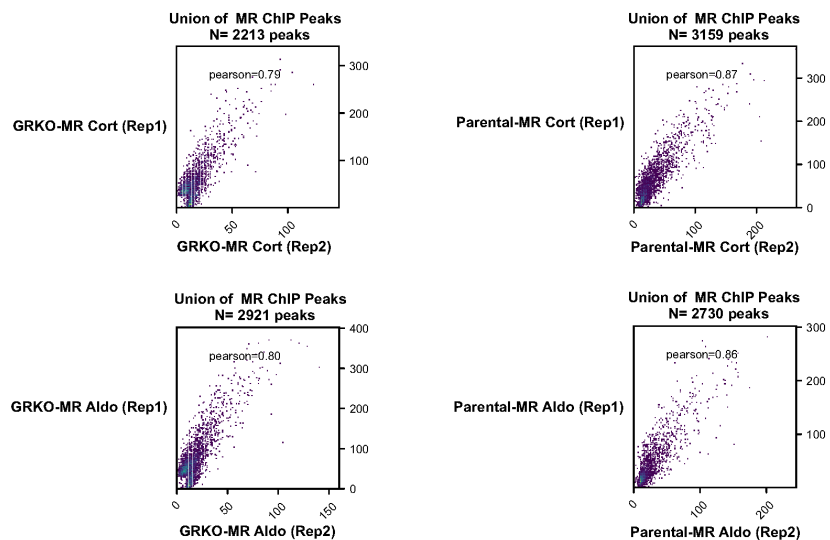


Figure S2. A-C. Pearson correlation of total RNA-seq replicates for each condition (cell type and hormone treatment). **A.** Adenocarcinoma GRKO cell line treated with vehicle, 100nM Cort or 10nM Aldo, three replicates each. **B.** Parental Adenocarcinoma cell line with endogenous GR treated with vehicle, 100nM Cort or 10nM Aldo, two to three replicates each. **C.** Mouse colon epithelial organoid cells (WT and Inducible GRKO) treated with vehicle or 10nM Aldo, five to six replicates each. **D.** Pearson correlation of called MR ChIP-seq peaks (hormone/veh, see Methods) from adenocarcinoma cell lines treated with 100nM Cort or 10nM Aldo, two replicates each.

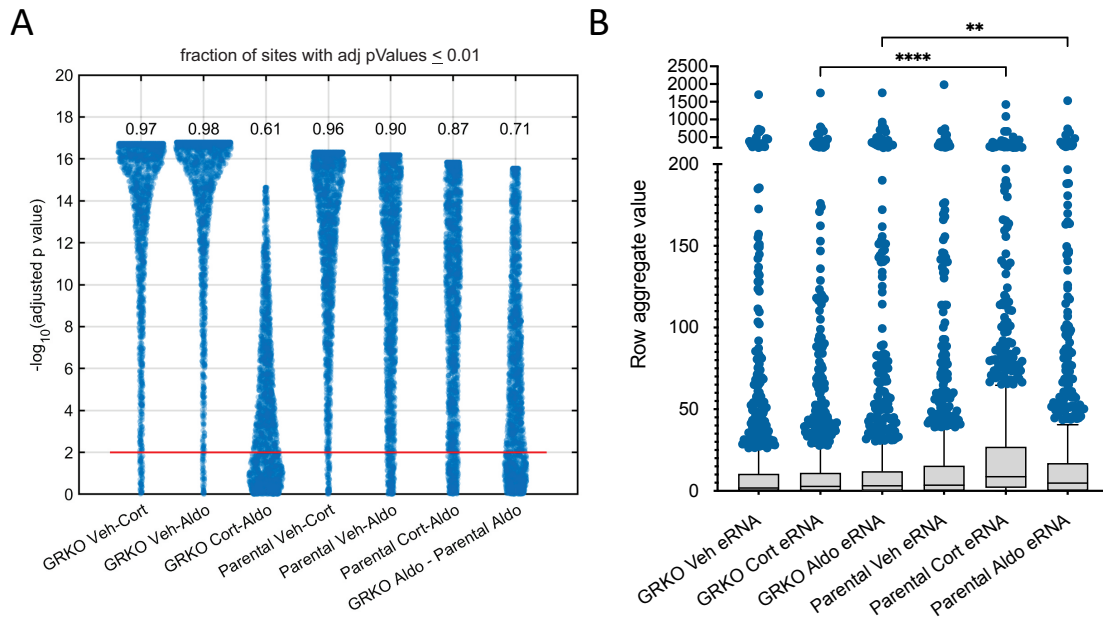


Figure S3. A. Swarmcharts represent the distributions of adjusted p-values obtained from pairwise comparison of ChIP-seq peaks in the indicated conditions using the paired Wilcoxon signed rank test, followed by the Benjamini and Hochberg correction for multiple comparisons. This analysis was used to test whether peaks were significantly different between each indicated pair of conditions. An adjusted p-value threshold of 0.01 was used to identify sites with significantly different MR binding (dots above the red line in the graph). Numbers above each dot cloud indicates the fraction of MR peaks in each condition that are significantly different between GRKO and parental cells. **B.** Box-whisker plots showing the aggregate value for each row in eRNA clusters 5.1-7.1 (main text, Fig.4). Statistical analysis was performed with Kruskal-Wallis test followed by Dunn's multiple comparison test (**, $p < 0.001$; ***, $p < 0.0001$). Only the two most relevant selected pairwise comparisons (GRKO-Cort vs. parental-Cort; GRKO-Aldo vs. parental-Aldo) are presented for the sake of simplicity.

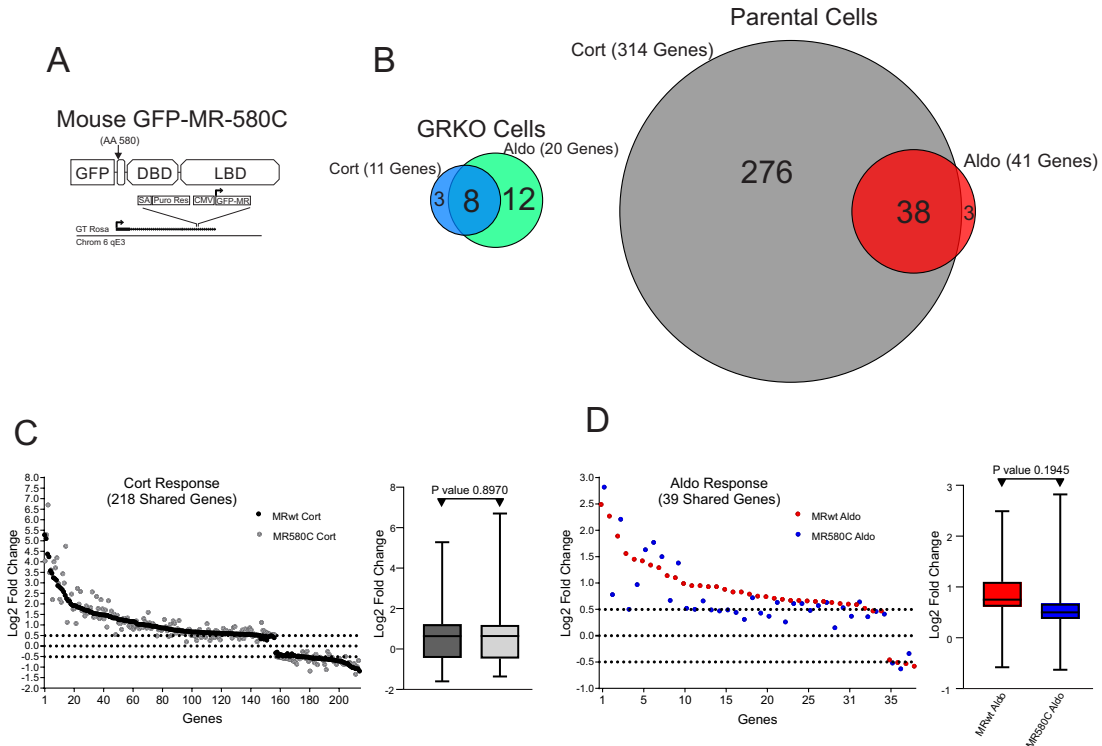


Figure S4. Contribution of MR N-terminal domain to the transcriptional response. A. Schematic diagram of the stably expressed MR NTD mutant. **B.** Venn diagrams of hormone-regulated protein-coding genes (2 h treatment/vehicle) to 100 nM Cort or 10 nM Aldo. Three replicates were used per condition. The number of hormone responsive genes ($FDR \leq 0.01$, $\text{Log}_2 \text{FC} \geq \pm 0.5$) denoted in parentheses for MR expressing GRKO cells or MR expressing parental cells (with endogenous GR). **C.** Scatter plot of $\text{Log}_2 \text{FC}$ for all shared Cort-responsive genes in the parental cells meeting the $FDR 0.01$ cutoff for MRwt (Fig. 1A) and MR580C, regardless of fold change. Box and whiskers plot of the same data displays interquartile range (IQR) depicting the 25th, 50th and 75th percentile as box with the median as black bar. The whiskers mark the most induced and repressed genes. **D.** Scatter and Box and Whiskers plots of $\text{Log}_2 \text{FC}$ for all shared Aldo-responsive genes in the parental cells, as described in panel C. Statistical analysis was performed using two-tailed non-parametric t test.

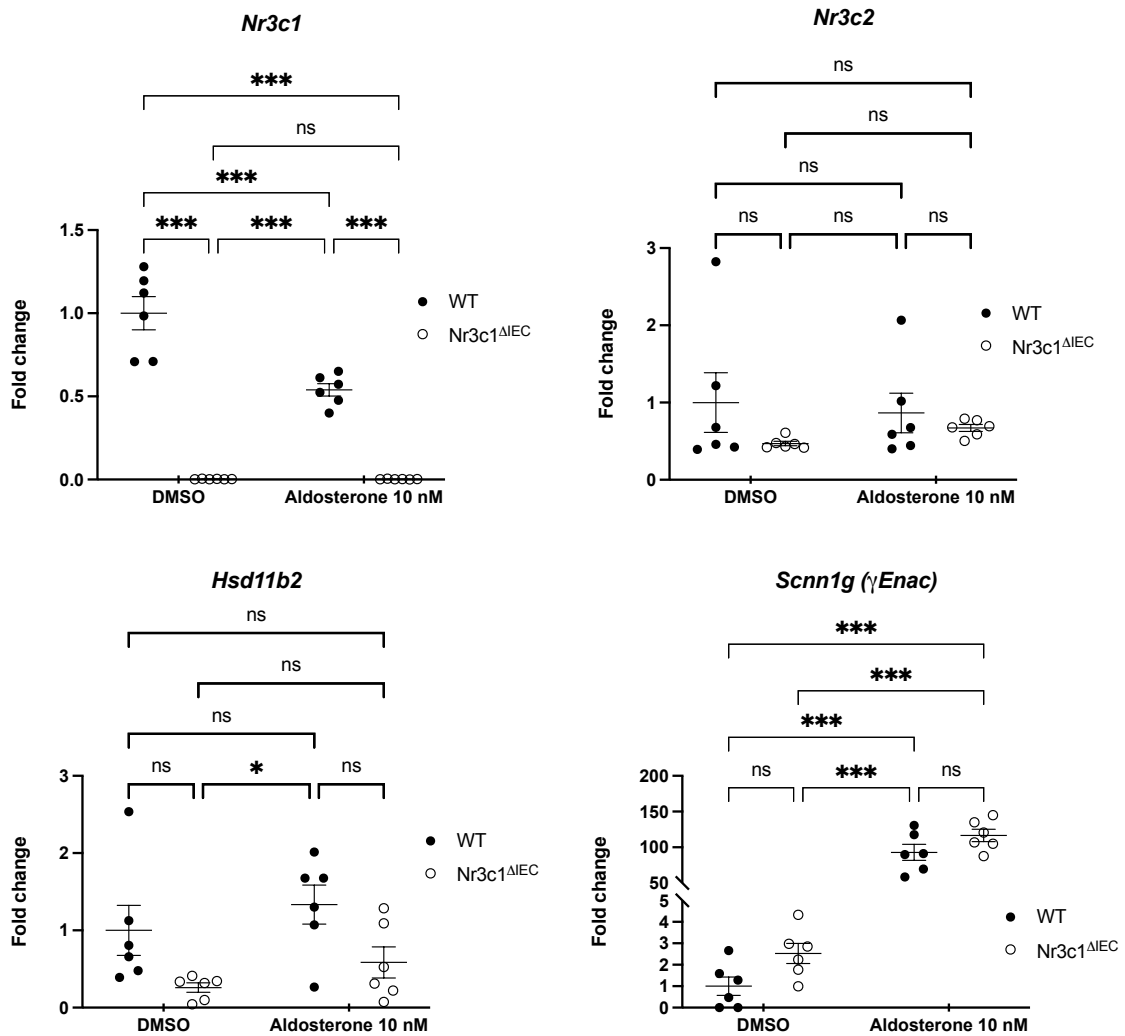


Figure S5. qPCR analysis of MR, GR, 11 β -HSD2 and mRNA abundance in colon organoids. Plots show relative mRNA abundance normalized to vehicle-treated wild type organoids. Each point represents a biological replicate; bars represent average \pm SE (N = 6). Statistical analysis was performed using two-way ANOVA followed by Tukey's multiple comparison test (*, $p < 0.05$; ***, $p < 0.001$).

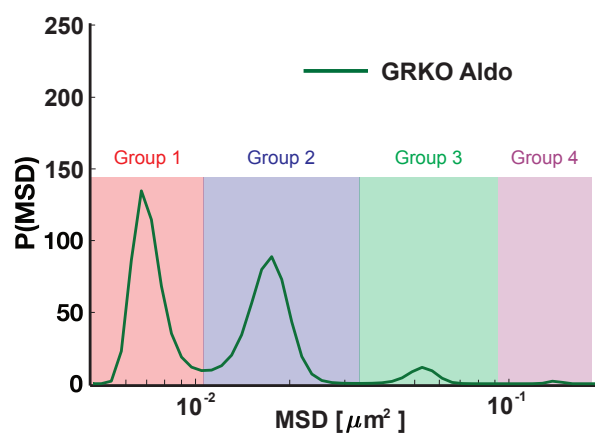


Figure S6. Identification of different mobility groups from the MSD distribution. A. representative mean squared displacement (MSD) distribution obtained by iteratively fitting the van Hove correlation function is shown. The local minima can be used to identify four distinct mobility groups.

Supplementary Table S1. Oligonucleotides used in this study

<i>18s</i>	F	ACACGGACAGGATTGACAGATTG
	R	GCCAGAGTCTCGTTCGTTATCG
<i>Hprt</i>	F	AGGGATTTGAATCACGTTTG
	R	TTTACTGGCAACATCAACAG
<i>Ppib</i>	F	TGGAGATGAATCTGTAGGAC
	R	CAAATCCTTTCTCTCCTGTAG
<i>Nr3c2</i>	F	CCAGAAGAGGGGACCACATA
	R	GGAATTGTGTAGCCTGCAT
<i>Nr3c1</i>	F	CAAGCCCTGGAATGAGACCA
	R	GCACAAAGGTAATTGTGCTGTC
<i>Hsd11b2</i>	F	CTGGATCGCGTTGTCCCGC
	R	AATCCAACACAGTGGCCAGCA
<i>Scnn1g</i>	F	CGGAAGCGGAAAATCAGCGG
	R	GAAGGTGTAGGTGGCGCAGT

Supplementary Table S2. Confidence intervals (CI) for each population fraction in the four different mobility states shown in main Figure 6. CI shown are the average of the upper and lower CI bounds. Fractions are expressed as % of total for each mobility state.

<i>Group</i>	State 1		State 2		State 3		State 4	
	<i>Fraction</i>	<i>95% CI (±)</i>	<i>Fraction</i>	<i>95% CI (±)</i>	<i>Fraction</i>	<i>95% CI (±)</i>	<i>Fraction</i>	<i>95% CI (±)</i>
GRKO Aldo	32.9	2.1	51.3	2.3	12.8	1.5	2.9	0.8
Parental Aldo	75.9	1.7	21.0	1.7	3.1	0.7	0.0	0.0
GRKO Cort	52.0	2.2	40.2	2.1	6.9	1.1	1.0	0.5
Parental Cort	47.2	2.2	45.4	2.2	6.6	1.1	0.7	0.4